









GRB241107A: a Giant Flare from a close-by extragalactic Magnetar?

JAMES CRAIG RODI ¹, DOMINIK PATRYK PACHOLSKI ^{2,3}, SANDRO MEREGHETTI ², EDOARDO ARRIGONI ^{2,3},
ANGELA BAZZANO ¹, LORENZO NATALUCCI ¹, RUBEN SALVATERRA ² AND PIETRO UBERTINI ¹

¹INAF - Istituto di Astrofisica e Planetologia Spaziali di Roma, Via del Fosso del Cavaliere 100, 00133 Roma, Italy

²INAF - Istituto di Astrofisica Spaziale e Fisica Cosmica di Milano, Via A. Corti 12, 20133 Milano, Italy

³Università degli Studi di Milano Bicocca, Dipartimento di Fisica G. Occhialini, Piazza della Scienza 3, 20126 Milano, Italy

ABSTRACT

We report the results on the short gamma-ray burst GRB 241107A, obtained with the IBIS instrument on board the *INTEGRAL* satellite. The burst had a duration of about 0.2 s, a fluence of 8×10^{-7} erg cm⁻² in the 20 keV-10 MeV range and a hard spectrum, characterized by a peak energy of 680 keV. The position of GRB 241107A has been precisely determined because it fell inside the imaging field of view of the IBIS coded mask instrument. The presence of the nearby galaxy PGC 86046 in the 3 arcmin radius error region, suggests that GRB 241107A might be a giant flare from a magnetar rather than a canonical short GRB. For the 4.1 Mpc distance of PGC 86046, the isotropic energy of 1.6×10^{45} erg is in agreement with this hypothesis, that is also supported by the time resolved spectral properties similar to those of the few other extragalactic magnetars giant flares detected so far.

1. INTRODUCTION

Since the time of the discovery of the first giant flare from a magnetar on 1979 March 5 (Mazets et al. 1979), it was realized that these energetic events ($L_{peak} = 10^{45-47}$ erg s⁻¹) can be detected up to distances of several Mpc by current hard X-ray / γ -ray instruments (Mazets et al. 1982). However, the long X-ray tails periodically modulated by the magnetar rotation that characterize the only three confirmed magnetar giant flares (MGFs), are too faint to be detected from sources located in galaxies farther than the Magellanic Clouds, making such events virtually undistinguishable from short gamma-ray bursts (sGRB).

Despite this difficulty, a few candidate extragalactic MGFs have been identified among short GRBs positionally consistent with nearby galaxies, often characterized by a high star formation rate (Frederiks et al. 2007; Mazets et al. 2008; Svinkin et al. 2021; Burns et al. 2021). The most recent example is 231115A (Mereghetti et al. 2024b), associated to the starburst galaxy M82 thanks to a localization with arcmin precision provided in real time by the INTEGRAL Burst Alert System (Mereghetti et al. 2003).

However, the sample of extragalactic MGFs candidates is still rather small, considering that these events are expected to account for a significant fraction of the population of short GRBs, with different estimates ranging from a few percent to a much larger fraction (Hurley et al. 2005; Nakar et al. 2006; Ofek 2007; Svinkin et al. 2015; Beniamini et al. 2024). Considering the low rate of giant flares at galactic (Milky Way and Magellanic Clouds) distances (only three observed in 50 years), it is clear that increasing the sample of extragalactic MGFs is the most promising way to acquire more information on the rate of these events, which, among other things, is relevant to understand the magnetic field evolution of magnetars.

The short GRB 241107A was first found in data from the *SVOM* and *INTEGRAL* satellites (SVOM/GRM Team et al. 2024; Rodi et al. 2024). An error box with area of about one square degree was obtained by triangulation of data from SVOM, INTEGRAL, Konus-WIND and Swift (Kozyrev et al. 2024). The only reported optical follow-up observation was performed 4.8 days after the trigger with the GROWTH-India Telescope, which derived upper limits of about 20.8 and 20.6 mag for r' and i' filters, respectively (Mohan et al. 2024). Although the burst was inside the fields of view of the INTEGRAL/IBIS and Swift/BAT imaging instruments, it was too faint to trigger the automatic burst searches. The offline analysis of these data provided positions with uncertainties of a few square arcmin (Mereghetti et al.

2024a; DeLaunay et al. 2024) at coordinates consistent with those of the galaxy PGC 86046. Here we report on the *INTEGRAL* observations of GRB 241107A and discuss its possible interpretation as a MGF candidate in this nearby galaxy ($D = 4.1_{-0.9}^{+1.2}$ Mpc, Tully et al. (2016)).

2. OBSERVATIONS AND DATA ANALYSIS

The IBIS imaging telescope (Ubertini et al. 2003) consists of two detectors operating simultaneously in different energy ranges. The *INTEGRAL* Soft Gamma-Ray Imager (ISGRI) provides photon-by-photon data in the 15-1000 keV range (Lebrun et al. 2003), while the Pixelised CsI Telescope (PICsIT) covers the 175 keV – 10 MeV range, providing images and light curves integrated in different energy and time bins (Labanti et al. 2003).

In the following analysis, we used PICsIT data in spectral-timing mode, which have a time resolution of 3.9 ms with counts integrated over the entire detector in 8 pre-defined energy channels from 212 keV to 2.6 MeV. Therefore, no imaging information is available for this data type. The background count rate in each energy channel was taken to be the median count rate during the *INTEGRAL* pointing (1800 s) including GRB 241107A. To account for the angular distance between GRB 241107A and the IBIS pointing direction (11.6 degrees), a correction was applied to the PICsIT effective area. This procedure is the same that was also used in the analysis of GRB 231115A (Mereghetti et al. 2024b).

2.1. Position of the burst

We used version 11.2 of the Off-line Scientific Analysis (OSA, Goldwurm et al. 2003) software to extract an image with the ISGRI data (no imaging information with adequate time resolution is provided by PICsIT). The burst is detected with the highest significance (6.7σ) by selecting data in the 30-180 keV energy range and in the time interval from $T_0+0.17$ s to $T_0+0.40$ s (with $T_0=2024-11-07$ 23:30:00 UTC). The derived coordinates are R.A. = 111.3360 deg, Dec. = -24.4439 deg (J2000) with an uncertainty of 3 arcmin (90% c.l. radius). This position is consistent with, and supersedes, the one derived using the preliminary satellite attitude information (Mereghetti et al. 2024a). Fig. 1 shows the error region of GRB 241107A superimposed on an optical image from Pan-STARRS1 (Chambers et al. 2016), where the PGC 86046 galaxy is clearly visible.

2.2. Timing and spectral properties

The light curves of GRB 241107A as measured by IBIS in different energy ranges are plotted in Fig. 2. The

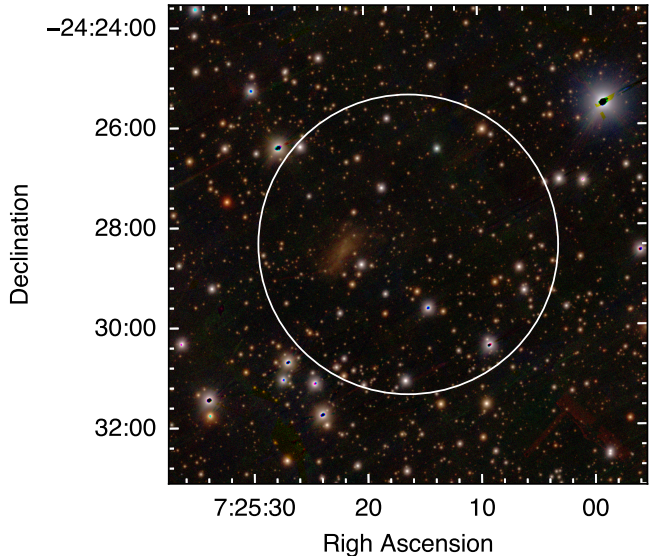


Figure 1. Pan-STARRS1 optical image of the location of GRB 241107A with the i-band, r-band, and g-band used as RGB colours. The circle with radius 3 arcmin is the IBIS/ISGRI position (90% c.l.). The galaxy PGC 86046 is clearly visible at coordinates R.A.=7:25:22, Dec.=−24:28:23

burst had a total duration of ~ 250 ms and consisted of an initial pulse lasting ~ 50 ms followed by a fainter tail. An image extracted from the ISGRI data in the time interval from $T_0+0.25$ s to $T_0+0.40$ s confirms that the tail is indeed due to the burst. Based on the PICsIT light curve, the GRB rise occurred within a single time bin and thus it lasted less than 3.9 ms.

The time averaged spectrum of GRB 241107A, obtained from the ISGRI and PICsIT data of the whole duration of the burst, is shown in Fig. 3. A good fit is found with an exponentially cut off power law model with photon index $\alpha = 0.07_{-0.24}^{+0.27}$, peak energy $E_p = 678_{-90}^{+125}$ keV and 20 keV – 10 MeV flux of $(3.4 \pm 0.5) \times 10^{-6}$ erg cm $^{-2}$ s $^{-1}$. This corresponds to a fluence of $\sim 8 \times 10^{-7}$ erg cm $^{-2}$. A single blackbody model gives a temperature of $kT = 136_{-11}^{+15}$ keV, but the fit is worse. All the fit parameters are given in Table 1.

We also extracted ISGRI and PICsIT spectra for two time intervals corresponding to the main pulse and the tail. Although the best fit parameters have relatively large uncertainties, they seem to indicate that the spectrum of the tail is slightly softer than that of the peak (see Table 1). As it is shown by the contour plots of the errors on α and E_p shown in Fig. 4, the spectral variation can be described by a reduction in the peak energy, rather than by a change in α .

To further investigate the burst spectral evolution we split the PICsIT data into the five time intervals indi-

Table 1. Results of Spectral Fits

Interval	Start-Stop ^a [s]	Model ^b	α	E_p [keV]	T_{BB} [keV]	Flux ^c [10^{-6} erg cm $^{-2}$ s $^{-1}$]	χ^2 (dof)
Total	0.17–0.40	CPL	$0.07^{+0.27}_{-0.24}$	678^{+125}_{-90}	–	3.4 ± 0.5	8.8(9)
		BB	–	–	136^{+15}_{-11}	$2.7^{+0.4}_{-0.2}$	21.8(10)
Peak	0.17–0.20	CPL	$0.71^{+0.42}_{-0.31}$	674^{+85}_{-71}	–	$16.1^{+1.9}_{-1.8}$	14.3(9)
		BB	–	–	152^{+18}_{-9}	$14.7^{+1.4}_{-1.5}$	17.0(10)
Tail	0.20–0.40	CPL	$-0.02^{+0.48}_{-0.39}$	460^{+126}_{-88}	–	1.1 ± 0.2	13.9(8)
		BB	–	–	99^{+22}_{-20}	1.0 ± 0.2	19.3(9)
1	0.1700–0.1765	CPL	0.07^d	352 ± 76		8^{+2}_{-2}	4.75(5)
2	0.1765–0.1882	CPL	0.07^d	579 ± 76		24^{+5}_{-4}	9.80(5)
3	0.1882–0.2038	CPL	0.07^d	889 ± 140		25^{+8}_{-6}	5.00(5)
4	0.2038–0.2155	CPL	0.07^d	679 ± 172		9^{+3}_{-2}	3.10(5)
5	0.2155–0.4000	CPL	0.07^d	499 ± 211		$0.6^{+0.4}_{-0.3}$	4.36(4)

NOTE—

^aTimes referred to T_0 ^bCPL = cutoff power law, BB = blackbody^cin the 20 keV – 10 MeV energy range^dfixed

cated in Table 1 and performed a joint fit to an exponentially cutoff power law with α fixed to the time-averaged value (0.07). We found that at the start of the burst E_p increases from ~ 330 keV to a maximum value of ~ 890 keV at the peak before decreasing to roughly 500 keV as the flux decays though the errors on the E_p values are large (see bottom panel of Figure 2 and Table 1).

The sky position of GRB 241107A was repeatedly observed by *INTEGRAL* starting from February 2003 to $T_0 + 5.7$ days. We extracted from the public data archive all the relevant IBIS pointings, totalling 9 Ms of exposure. Using the method described in [Mereghetti et al. \(2021\)](#) and [Pacholski et al. \(2024\)](#), we searched for other possible bursts from this position, but none was found.

3. DISCUSSION AND CONCLUSIONS

The short duration and hard spectrum of GRB 241107A are consistent with the properties of short GRBs, but its possible association with a nearby galaxy leads us to also consider the alternative interpretation in terms of a MGF.

The chance coincidence of finding a galaxy brighter than magnitude m in an error circle of radius R is given by

$$P(< m) = 1 - e^{-\pi R^2 \sigma(< m)} \quad (1)$$

where, $\sigma(< m)$ is the number density of galaxies brighter than m . We derived $\sigma(< m)$ from the galaxy number counts plotted in Fig. 4 of [Ferguson et al. \(2000\)](#) and used the PGC 86046 magnitudes in the I and B bands, $m_B = 16.336$, $m_I = 14.634$, reported in the HIPASS catalogue ([Doyle et al. 2005](#)). For $R=3$ arcmin, we ob-

tain chance coincidence probabilities of $P(< m_B)=2.9\%$ and $P(< m_I)=5.5\%$.

At the PGC 86046 distance of 4.1 Mpc ([Tully et al. 2016](#)), the fluence derived in Sec. 2.2 corresponds to an emitted isotropic energy $E_{iso} = 1.6 \times 10^{45}$ erg, that fits perfectly with the typical values of MGFs. This is illustrated in the $E_p - E_{iso}$ plot of Fig. 5, where the values of GRB 241107A for different assumed distances are compared with those of the other MGFs and of the short GRBs.

It is also interesting to compare GRB 241107A with the MGF candidate in the Sculptor Galaxy, GRB 200415A ([Svinkin et al. 2021](#); [Roberts et al. 2021](#)), which, in the small sample of extragalactic MGFs, is probably the one with the best spectral information. During the initial ~ 7 ms, its spectrum hardened, with E_p evolving from 430 keV to 1.8 MeV, and then it gradually softened with E_p tracing the downward flux evolution. A similar behavior is possibly seen also in GRB 231115A ([Trigg et al. 2024](#)), which is currently the most convincing extragalactic MGF and is associated to the M82 starburst galaxy ([Mereghetti et al. 2024b](#)). The spectral evolution of GRB 241107A shown in Fig. 2 is consistent with a similar behavior. These three bursts are also similar for their rise times $\lesssim 4$ ms and some evidence for a double-peaked light curve.

For GRB 200415A time-resolved analysis of the relationship between E_p and the isotropic luminosity (L_{iso}) found $E_p \propto L_{iso}^{0.23 \pm 0.10}$ ([Chand et al. 2021](#)). The authors report a stronger correlation with an exponent of 0.31 ± 0.04 when excluding the three spectra before

$T_0 - 0.001$ s. In the case of GRB 231115A, the exponent is $0.35^{+0.11}_{-0.07}$ or $0.41^{+0.21}_{-0.08}$ depending on the time binning (Trigg et al. 2024). A fit to our values for GRB 241107A has an exponent of 0.32 ± 0.15 , similar to that of the other two MGF candidates.

In conclusion, although we cannot exclude that GRB 241107A is an ordinary short GRB at redshift $\gtrsim 0.1$, its properties are consistent with a MGF origin, as it is suggested by the presence of a nearby galaxy with a chance probability of only a few percent of being in the burst error region. Unfortunately, GRB 241107A could not be localized precisely in near real time. Rapid follow-up observations at other wavelengths could have provided compelling evidence in favor of one of the two possibilities for the nature of GRB 241107A.

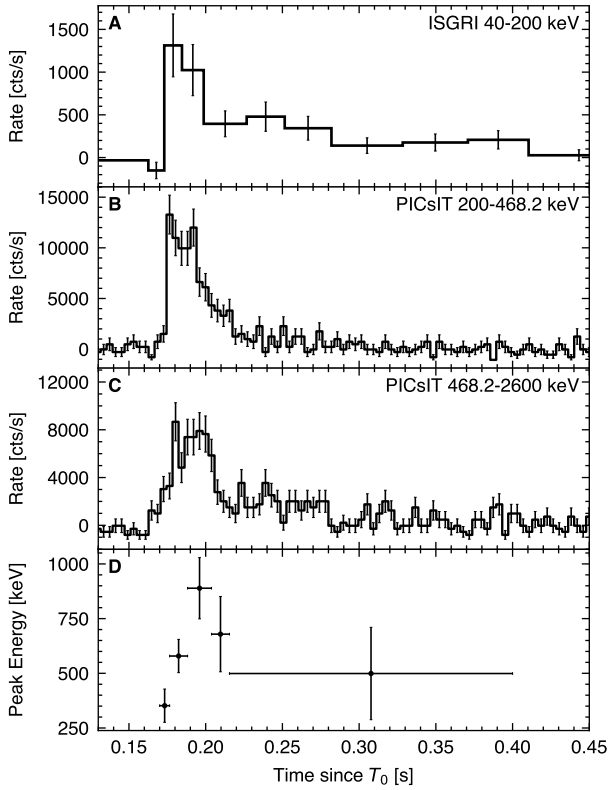


Figure 2. Background subtracted light curves of GRB 241107A in three energy bands, with $T_0=2024-11-07$ 23:30:00 UT. The ISGRI (40-200 keV) light curve has been binned to have at least 18 counts in each bin (A panel). The PICsIT light curves (200-468.2 keV, B panel and 468.2-2600 keV, C panel) have the original bin size of 3.9 ms. Panel D shows the evolution of E_p during the burst.

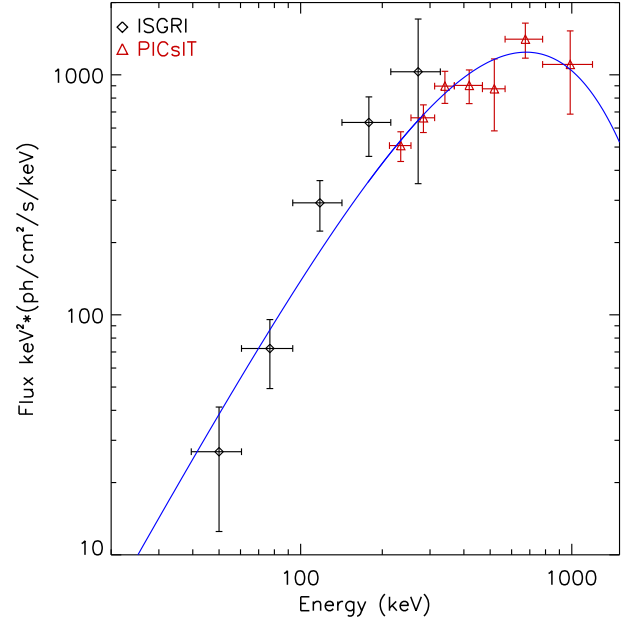


Figure 3. Time averaged IBIS spectrum of GRB 241107A (from $T_0+0.17$ s to $T_0+0.40$ s). ISGRI data are plotted as black diamonds and PICsIT data as red triangles. The best fit cutoff power-law model is overplotted as a solid blue line.

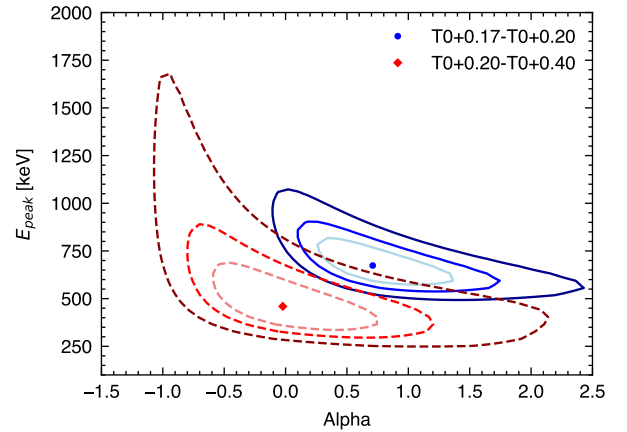


Figure 4. Confidence contours of the joint ISGRI+PICsIT spectra for the peak ($T_0+0.17$ - $T_0+0.20$, solid blue line) and tail ($T_0+0.20$ - $T_0+0.40$, dashed red line) of the burst. The contours represent confidence levels of 68%, 90%, and 99%.

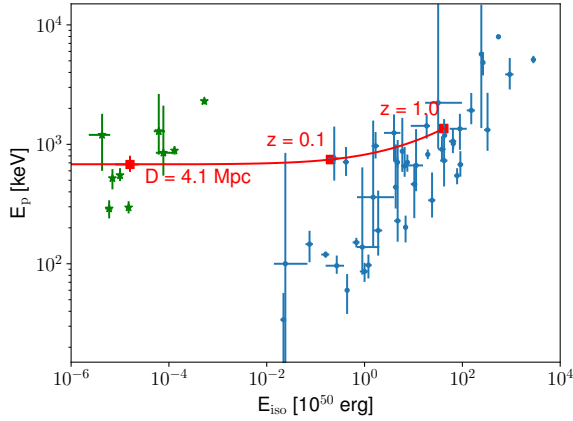


Figure 5. Position of GRB 241107A (red square) in the E_p versus E_{iso} plane. The sample of short GRBs (blue) is taken from Minaev & Pozanenko (2020). The three confirmed magnetar giant flares and the extragalactic MGF candidates are indicated by the green stars (data from Pacholski et al. (2024) and references therein and Svinkin et al. (2016)).

REFERENCES

- Beniamini, P., Wadiasingh, Z., Trigg, A., et al. 2024, arXiv e-prints, arXiv:2411.16846, doi: [10.48550/arXiv.2411.16846](https://doi.org/10.48550/arXiv.2411.16846)
- Burns, E., Svinkin, D., Hurley, K., et al. 2021, ApJL, 907, L28, doi: [10.3847/2041-8213/abd8c8](https://doi.org/10.3847/2041-8213/abd8c8)
- Chambers, K. C., Magnier, E. A., Metcalfe, N., et al. 2016, arXiv e-prints, arXiv:1612.05560, doi: [10.48550/arXiv.1612.05560](https://doi.org/10.48550/arXiv.1612.05560)
- Chand, V., Joshi, J. C., Gupta, R., et al. 2021, Research in Astronomy and Astrophysics, 21, 236, doi: [10.1088/1674-4527/21/9/236](https://doi.org/10.1088/1674-4527/21/9/236)
- DeLaunay, J., Tohuvavohu, A., Ronchini, S., et al. 2024, GRB Coordinates Network, 38177, 1
- Doyle, M. T., Drinkwater, M. J., Rohde, D. J., et al. 2005, MNRAS, 361, 34, doi: [10.1111/j.1365-2966.2005.09159.x](https://doi.org/10.1111/j.1365-2966.2005.09159.x)
- Ferguson, H. C., Dickinson, M., & Williams, R. 2000, ARA&A, 38, 667, doi: [10.1146/annurev.astro.38.1.667](https://doi.org/10.1146/annurev.astro.38.1.667)
- Frederiks, D. D., Palshin, V. D., Aptekar, R. L., et al. 2007, Astronomy Letters, 33, 19, doi: [10.1134/S1063773707010021](https://doi.org/10.1134/S1063773707010021)
- Goldwurm, A., David, P., Foschini, L., et al. 2003, A&A, 411, L223, doi: [10.1051/0004-6361:20031395](https://doi.org/10.1051/0004-6361:20031395)
- Hurley, K., Boggs, S. E., Smith, D. M., et al. 2005, Nature, 434, 1098, doi: [10.1038/nature03519](https://doi.org/10.1038/nature03519)
- Kozyrev, A. S., Golovin, D. V., Litvak, M. L., et al. 2024, GRB Coordinates Network, 38165, 1
- Labanti, C., Di Cocco, G., Ferro, G., et al. 2003, A&A, 411, L149, doi: [10.1051/0004-6361:20031356](https://doi.org/10.1051/0004-6361:20031356)
- Lebrun, F., Leray, J. P., Lavocat, P., et al. 2003, A&A, 411, L141, doi: [10.1051/0004-6361:20031367](https://doi.org/10.1051/0004-6361:20031367)
- Mazets, E. P., Golenetskii, S. V., Gurian, I. A., & Ilinskii, V. N. 1982, Ap&SS, 84, 173, doi: [10.1007/BF00713635](https://doi.org/10.1007/BF00713635)
- Mazets, E. P., Golenskii, S. V., Ilinskii, V. N., Aptekar, R. L., & Guryan, I. A. 1979, Nature, 282, 587, doi: [10.1038/282587a0](https://doi.org/10.1038/282587a0)
- Mazets, E. P., Aptekar, R. L., Cline, T. L., et al. 2008, ApJ, 680, 545, doi: [10.1086/587955](https://doi.org/10.1086/587955)
- Mereghetti, S., Götz, D., Borkowski, J., Walter, R., & Pedersen, H. 2003, A&A, 411, L291, doi: [10.1051/0004-6361:20031289](https://doi.org/10.1051/0004-6361:20031289)
- Mereghetti, S., Pacholski, D. P., Gotz, D., et al. 2024a, GRB Coordinates Network, 38172, 1
- Mereghetti, S., Topinka, M., Rigoselli, M., & Götz, D. 2021, ApJL, 921, L3, doi: [10.3847/2041-8213/ac2ee7](https://doi.org/10.3847/2041-8213/ac2ee7)
- Mereghetti, S., Rigoselli, M., Salvaterra, R., et al. 2024b, Nature, 629, 58, doi: [10.1038/s41586-024-07285-4](https://doi.org/10.1038/s41586-024-07285-4)
- Minaev, P. Y., & Pozanenko, A. S. 2020, MNRAS, 492, 1919, doi: [10.1093/mnras/stz3611](https://doi.org/10.1093/mnras/stz3611)
- Mohan, T., Waratkar, G., Saikia, A. P., et al. 2024, GRB Coordinates Network, 38187, 1
- Nakar, E., Gal-Yam, A., Piran, T., & Fox, D. B. 2006, ApJ, 640, 849, doi: [10.1086/498229](https://doi.org/10.1086/498229)
- Ofek, E. O. 2007, ApJ, 659, 339, doi: [10.1086/511147](https://doi.org/10.1086/511147)

- Pacholski, D. P., Arrigoni, E., Mereghetti, S., & Salvaterra, R. 2024, MNRAS, doi: [10.1093/mnras/stae2517](https://doi.org/10.1093/mnras/stae2517)
- Roberts, O. J., Veres, P., Baring, M. G., et al. 2021, Nature, 589, 207, doi: [10.1038/s41586-020-03077-8](https://doi.org/10.1038/s41586-020-03077-8)
- Rodi, J., Ubertini, P., Bazzano, A., & Natalucci, L. 2024, GRB Coordinates Network, 38164, 1
- Svinkin, D., Frederiks, D., Hurley, K., et al. 2021, Nature, 589, 211, doi: [10.1038/s41586-020-03076-9](https://doi.org/10.1038/s41586-020-03076-9)
- Svinkin, D. S., Hurley, K., Aptekar, R. L., Golenetskii, S. V., & Frederiks, D. D. 2015, MNRAS, 447, 1028, doi: [10.1093/mnras/stu2436](https://doi.org/10.1093/mnras/stu2436)
- Svinkin, D. S., Frederiks, D. D., Aptekar, R. L., et al. 2016, ApJS, 224, 10, doi: [10.3847/0067-0049/224/1/10](https://doi.org/10.3847/0067-0049/224/1/10)
- SVOM/GRM Team, Wang, C.-W., Zheng, S.-J., et al. 2024, GRB Coordinates Network, 38125, 1
- Trigg, A. C., Stewart, R., van Kooten, A., et al. 2024, arXiv e-prints, arXiv:2409.06056, doi: [10.48550/arXiv.2409.06056](https://doi.org/10.48550/arXiv.2409.06056)
- Tully, R. B., Courtois, H. M., & Sorce, J. G. 2016, AJ, 152, 50, doi: [10.3847/0004-6256/152/2/50](https://doi.org/10.3847/0004-6256/152/2/50)
- Ubertini, P., Lebrun, F., Di Cocco, G., et al. 2003, A&A, 411, L131, doi: [10.1051/0004-6361:20031224](https://doi.org/10.1051/0004-6361:20031224)